Journal of Alzheimer's Disease xx (2023) x–xx
DOI 10.3233/JAD-220843
IOS Press

Inferior Frontal Sulcal Hyperintensity on FLAIR Is Associated with Small Vessel Disease but not Alzheimer's Disease Pathology

Shan Xu[1], Linyun Xie[1], Yao Zhang, Xiao Wu, Hui Hong, Ruiting Zhang, Qingze Zeng, Kaicheng Li, Xiao Luo, Minming Zhang, Jianzhong Sun* and Peiyu Huang[a,*]and for behalf of Alzheimer's Disease Neuroimaging Initiative (ADNI)[2]
Department of Radiology, The Second Affiliated Hospital, Zhejiang University School of Medicine, Hangzhou, China

Accepted 8 February 2023
Pre-press 6 March 2023

Abstract.
Background: The inferior frontal sulci are essential sites on the route of cerebrospinal fluid outflow. A recent study suggests that inferior frontal sulcal hyperintensities (IFSH) on FLAIR images might be related to glymphatic dysfunction.
Objective: To investigate whether IFSH is associated with Alzheimer's disease (AD) pathology and cerebral small vessel disease (SVD) burden.
Methods: We retrospectively collected data from 272 non-demented subjects in the ADNI3 database. The IFSH was assessed on 3D fluid-attenuated inversion recovery images. The standardized uptake value ratios of amyloid and tau PET were used to reflect the AD pathology burden. To measure the SVD burden, we assessed white matter hyperintensities (WMH), dilation of perivascular spaces, microbleeds, and lacunes. Finally, we performed ordinal logistic regression analyses to investigate the associations between the IFSH score and AD pathology and SVD burden.
Results: The IFSH score was associated with the deep WMH score (OR, 1.79; 95% CI, 1.24 – 2.59) controlling for age and sex. The association remained significant in the multivariable regression models. There was no association between the IFSH score and AD pathology burden.

[1]These authors contributed equally to this work.

*Correspondence to: Dr. Peiyu Huang, and Dr. Jianzhong Sun, Department of Radiology, The Second Affiliated Hospital, Zhejiang University School of Medicine, No.88 Jiefang Road, Shangcheng District, Hangzhou, 310009, China, Phone: +86 0571 87315255; Fax: +86 0571 87315255; E-mail: huangpy@zju.edu.cn. (Peiyu Huang); and E-mail: 2191009@zju.edu.cn. (Jianzhong Sun).

[2]Data used in preparation of this article were obtained from the Alzheimer's Disease. Neuroimaging Initiative (ADNI) database (http://adni.loni.usc.edu). As such, the investigators within the ADNI contributed to the design and implementation of ADNI and/or provided data but did not participate in analysis or writing of this report. A complete listing of ADNI investigators can be found at: https://adni.loni.usc.edu/wp-content/uploads/how_to_apply/ADNI_Acknowledgement_List.pdf

Conclusion: This study suggests that the IFSH sign is associated with SVD but not AD pathology. Further studies are needed to confirm the findings.

Keywords: Alzheimer's disease, inferior frontal sulcal hyperintensity, magnetic resonance imaging, small vessel disease, white matter hyperintensities

INTRODUCTION

The cerebrospinal fluid (CSF), usually dark on the fluid-attenuated inversion recovery (FLAIR) sequence, may become hyperintense in brain sulci under several disease conditions [1–3]. Aging-related glymphatic dysfunction [4] may cause the accumulation of waste proteins and cell debris in CSF, which can change CSF relaxation properties through the bound-water effect and lead to FLAIR hyperintensity. Zhang et al. [5] found that the inferior frontal sulcal hyperintensities (IFSH) on FLAIR images were associated with increased age, as well as the dilation of perivascular spaces (PVS), a presumed marker of glymphatic dysfunction [6]. Indeed, because the CSF flows through the inferior frontal sulci (IFS) and drains through the cribriform plate to nasal lymphatics [7], the IFS is a highly possible site for waste accumulation. A similar effect has also been observed in the parasagittal [8] dura, another glymphatic efflux site.

Based on their findings in community subjects and patients with small vessel disease (SVD), Zhang et al. proposed that the IFSH could be a non-invasive imaging marker of altered CSF clearance. Nevertheless, more studies are needed to confirm this novel finding. Furthermore, an intriguing question is whether this phenomenon exists in other disease conditions involving glymphatic dysfunction, e.g., Alzheimer's disease (AD). AD is closely associated with impaired waste clearance [9] and pathological protein deposition [10, 11]. Studies have shown that vascular lesions [12], amyloid-β (Aβ) deposition [13], insomnia [14], and other related factors may lead to glymphatic dysfunction in AD and promote disease progression. AD pathologies can also cause a higher waste production rate due to progressive neurodegeneration. Additionally, the frontal lobe, especially the orbitofrontal lobe [15], is a crucial region for Aβ deposition.

In the present study, we aim to investigate the association between IFSH and AD pathology burdens and SVD imaging markers in non-demented subjects from the Alzheimer's Disease Neuroimaging Initiative (ADNI) database. We hypothesize that the IFSH score is related to higher AD pathology burdens and SVD imaging markers.

MATERIALS AND METHODS

Alzheimer's Disease Neuroimaging Initiative

The data used in this study were downloaded from the ADNI3 database. ADNI was launched in 2004 and funded by 20 companies, the National Institutes of Health and the National Institute on Aging. The goals of the ADNI include: finding biomarkers for early AD diagnosis, tracking the pathology of the disease, and aiding the development of AD prevention and treatment methods. ADNI recruits participants across North America. During each phase of the study, it has collected a variety of biomarkers. Data in ADNI are shared through the USC Laboratory of Neuro Imaging's Image and Data Archive (IDA).

Subjects

We screened subjects from the ADNI3 database in early November of 2021. The inclusion criteria are: 1) non-demented subjects, including cognitively normal (CN) subjects and subjects with mild cognitive impairment (MCI); 2) having 3D T1 and FLAIR MRI data; 3) having amyloid PET data. All the demographic information, imaging data, and *APOE* genotype were downloaded from the database. We also collected axial T2* images and tau PET data when available.

Image acquisition and processing

MRI data were obtained using 3T scanners from multiple research centers. The ADNI3 MRI protocol has been harmonized across centers, but the sequence parameters will vary based on system hardware and software. The main parameters of sagittal 3D FLAIR images were: repetition time = 4800 s; echo time = 441 ms; inversion time = 1650 ms; voxel size = 1.2*1*1 mm^3. Parameters of FLAIR sequences

from different scanners were listed in Supplementary Table 1. T1-weighted images were acquired based on sagittal 3D accelerated Magnetization Prepared Rapid Acquisition Gradient Echo (MPRAGE) sequence. Representative parameters of T1 W images were: echo time = min full echo; repetition time = 2300 ms; inversion time = 900 ms; voxel size = 1*1*1 mm^3. Axial T2* images were acquired with a gradient recalled echo (GRE) sequence; the parameters were: repetition time = 650 ms; echo time = 20 ms; voxel size = 0.85*0.85*4 mm. In ADNI3, [18 F]-Florbetapir (Amyvid) and [18 F]-Florbetaben (Neuraceq) were used in amyloid PET imaging. Subjects had a 20-min dynamic scan consisting of four 5-min frames that started at either 50 min (florbetapir) or 90 min (florbetaben) post-injection. The tau PET imaging was performed with [18 F]-AV1451 at 75 min post-injection with a 30-min dynamic scan consisting of six 5-min frames. Details of the ADNI3 MRI and PET protocol are available online (https://adni.loni.usc.edu/methods/documents/).

Amyloid and tau PET analysis

We downloaded the tau PET and amyloid PET data from the ADNI3 database processed by the University of Berkeley. PET data were corrected for partial volume. The processing method included: 1) collecting pre-processed PET and MR data, 2) coregistration to MRI image, 3) definition of regions of interest and reference regions by FreeSurfer, 4) extraction of volume-weighted means from a cortical summary region (including frontal, anterior/posterior cingulate, lateral temporal regions) for amyloid PET analysis and Braak stage composite regions, meta-temporal regions for tau PET analysis, 5) calculation of the cortical summary SUVR by normalization the cortical summary region to the whole cerebellum with a threshold of 1.11; Calculation of Flortaucipir SUVR by dividing regions of interest (including Braak stage composite regions and meta-temporal regions) by inferior cerebellar gray matter with a threshold of 1.23. The detailed information about the processing method was online (https://ida.loni.usc.edu/pages/access/studyData.j).

Visual assessment of SVD imaging biomarkers

SVD imaging markers [16], including white matter hyperintensities (WMHs), lacunes, microbleeds, and perivascular spaces (PVS) were assessed by a post-graduate student with 6-year experience in radiology (SX).

The dilated PVS (dPVS) was evaluated on T1 images due to a lack of T2 images in the ADNI3 database. It was defined as a round, oval, or linear lesion with a maximum diameter < 3 mm and has a CSF-like signal (hypointense on T1), perpendicular to the brain surface and parallel to perforating vessels. We estimated the severity based on the number of dPVS with a rating scale of 0 to 4 in basal ganglia (BG) and centrum semiovale (CSO) separately [17] as follows: in basal ganglia, 0 = none, 1 = <5, 2 = 5–10, 3 = >10 and the number is still countable, 4 = the number is uncountable; in centrum semiovale, 0 = none, 1 = <10 in total, 2 = >10 in total but no more than 10 in a single slice, 3 = 10–20 in the slice containing the largest number, 4 = >20 in any single slice.

Lacune was defined as a small fluid-filled cavity with diameters ranging from 3 to 15 mm, which is round or oval, surrounded by a hyperintense rim on the FLAIR sequence. We counted the number directly based on FLAIR images.

CMBs were referred to as hypointense foci, notably at T2*-weighted or susceptibility-weighted (SW) imaging with diameters 2 to 5 mm generally, sometimes up to 10 mm. We counted the number of microbleeds from the T2*-weighted sequence. WMHs were defined as hyperintense on FLAIR or T2-weighted images without obvious hyperintense on T1-weighted images. We performed the visual rating of WMH according to Fazekas based on FLAIR images. The Fazekas scale rates WMH in both the periventricular (PWMH) and deep (DWMH) white matter on a 0-3-point scale, respectively [18].

Visual rating for IFSH

IFSH was defined as abnormal CSF hyperintense signals in one or more of the three inferior frontal sulci (the central sulcus, the left and right olfactory sulci) seen on 3D FLAIR images. We evaluated the degree of IFSH according to the scale proposed by Lim et al. [19]. Firstly, we re-orientated all FLAIR images parallel to the floor of the anterior cranial fossa by multi-planar reconstruction (MPR). Secondly, we identified the reference slice that clearly displayed all three sulci. Finally, we rated the IFSH score for each sulcus on images above the reference slice. Each sulcus was scored from 0 to 3:0 = none of the sulcus affected, 1 = less than half of sulcus length affected, 2 = at least half of sulcus length affected,

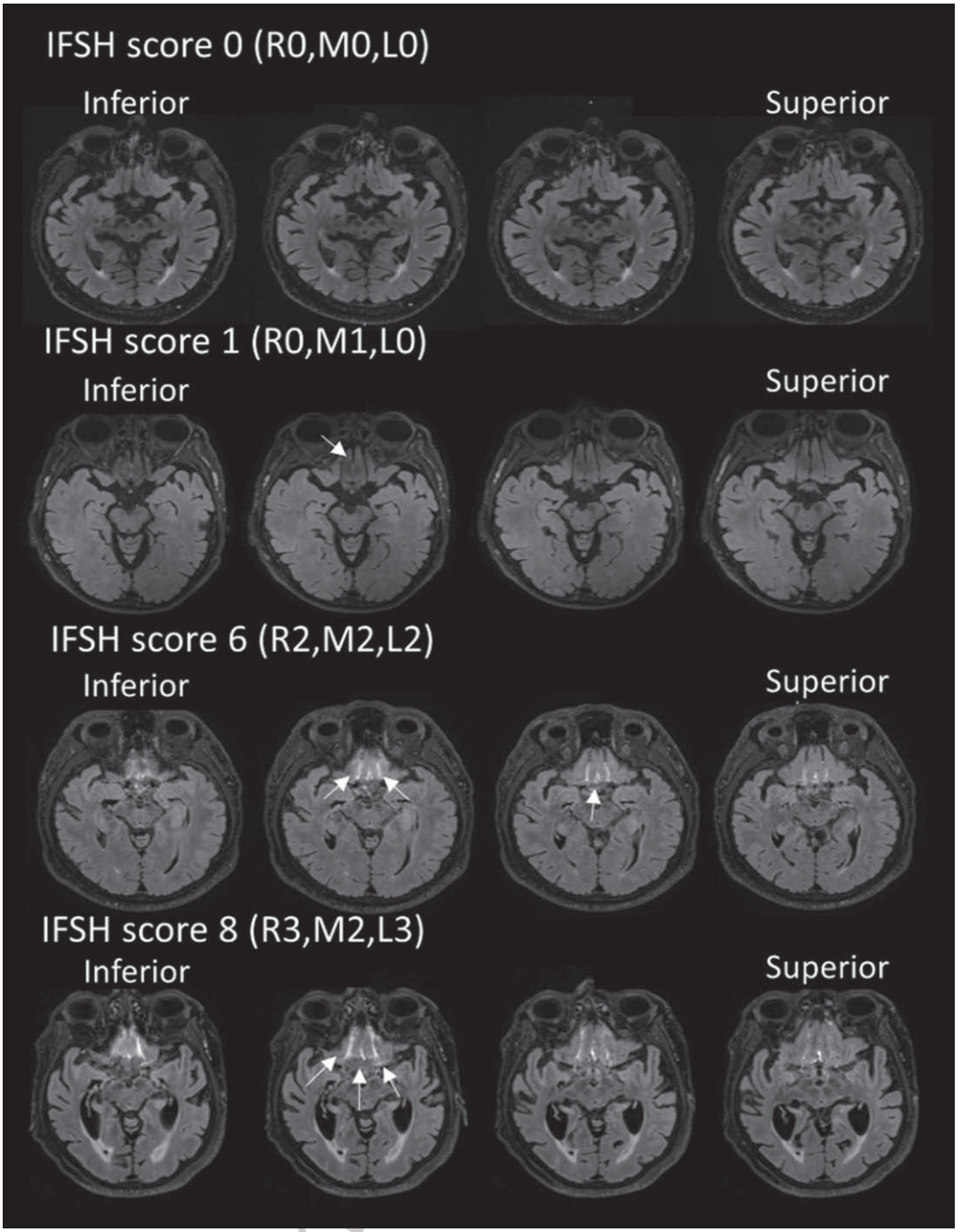

Fig. 1. IFSH rating examples. Examples of Inferior Frontal Sulcal Hyperintensity (IFSH) scores on FLAIR images. The IFSH score in each of the three inferior frontal sulci was evaluated on images above the reference slice (the left image in each row). Each sulcus was scored from 0 to 3:0 = non-affected, 1 = less than half of sulcus length affected, 2 = at least half of sulcus length affected, 3 = most or whole of sulcus length affected.

and 3 = most or whole of sulcus length affected. The overall IFSH score was the sum of the scores of the 3 sulci, ranging from 0 to 9 (Fig. 1). We categorized the total IFSH scores into three levels (0–1, 2–4, 5–9) according to the distribution of the scores in all subjects.

As the IFSH is a newly proposed imaging sign, two postgraduate students (LYX, 4-year experi-

ence in medical imaging; SX, 6-year experience in radiology), trained together and blinded to clinical information, evaluated the IFSH score. Cohen's kappa was used to assess the consistency between the results from the two raters. There were good agreements in the right sulci score (Kappa = 0.639), the left sulci score (Kappa = 0.678), the central sulci score (Kappa = 0.658), and the total IFSH score (Kappa = 0.522). Disagreements were solved by discussion.

Calculation of brain parenchymal fraction

We calculated the brain parenchymal fraction (brain-volume to total-intracranial-volume ratio, BrainVol/TIV) to reflect overall neurodegeneration. The FreeSurfer software was used to segment different brain tissue types based on T1-weighted images and to calculate TIV. The BrainVol/TIV was calculated by the formula: (gray matter volume + white matter volume) /TIV.

Statistical analysis

Age, amyloid PET SUVR, tau PET SUVR, BrainVol/TIV, and the number of lacunes and microbleeds were considered continuous variables. The category of the IFSH score, BG-PVS score, CSO-PVS score, and WMH score were considered categorical variables. All statistical analyses were performed in IBM SPSS 26.

Firstly, we performed univariate ordinal regression analyses. The category of the IFSH score was set as the dependent variable, and age, sex, *APOE* ε4 genotype, BrainVol/TIV, SVD markers, and AD biomarkers were set as independent variables separately (Model 1). Then, we re-performed the analyses controlling for age and sex (Model 2). Finally, we used multivariable ordinal regression models to investigate each factor's independent contribution to the category of the IFSH score. Age, sex, *APOE* ε4, BrainVol/TIV, SVD markers, and PET SUVRs were independent variables. In view of the prevalence of IFSH in different scanners (Supplementary Table 2), we also adjusted the scanner model in multivariable ordinal regression analyses. Because only 129 subjects had tau PET data, the analysis was performed twice, without or with tau PET SUVR (Model 3 and Model 4). Multi-collinearity was examined to avoid biased fitting. Odds ratios were used to reflect the degree of influence. The *p*-value for statistical significance was set at 0.05, 2-tailed.

RESULTS

Demographics

A total of 272 subjects (mean age $\pm$ SD = 78.0 $\pm$ 7.2, f/m = 132/140) were included in this study (Table 1), consisting of 107 CN (39.3%) and 165 MCI (60.7%). Among them, 245 had T2* images, 144 had tau-PET data, and 129 had both T2* images and tau-PET data. Among the four groups, there were no statistical differences in demographic characteristics, *APOE* ε4 genotype, IFSH score, BrainVol/TIV, SVD biomarkers, and AD biomarkers.

Association between IFSH and age, sex, APOE ε4 genotype, BrainVol/TIV

The IFSH score was negatively associated with the brain parenchymal fraction in the univariate regression analysis. However, the association diminished in the multivariable analyses (Table 2, Model 3, 95% CI, 1.00–1.25; Model 4, 95% CI, 0.88–1.26). There were no associations between the IFSH score and age, sex, and *APOE* ε4 genotype.

Association between IFSH and SVD markers, AD markers

Univariate regression analyses showed that the IFSH score was positively associated with the DWMH score (Table 2. Model 1, OR, 1.75; 95% CI, 1.24–2.47). The association remained significant after adjusting for age and sex (Model 2, OR, 1.79; 95% CI, 1.24–2.59). Amyloid and tau PET SUVR were not associated with the IFSH score.

In multiple regression analyses, the IFSH score was still associated with the DWMH score regardless of whether including the tau PET SUVR in the model (Model 4, OR, 3.02; 95% CI, 1.17–7.77) or not (Model 3, OR, 2.16; 95% CI, 1.12–4.17). The association between the IFSH score and CSO-PVS score was significant in Model 4 (OR 1.97; 95% CI, 1.09 – 3.57). The other SVD and AD markers were not associated with the IFSH score.

DISCUSSION

In the present study, we examined the association between the IFSH score, AD pathology burdens, and SVD imaging markers. We found that the IFSH score was negatively associated with the severity of DWMH. There was no association between the IFSH

Table 1
Subject characteristics

	Whole sample $n = 272$	Subjects with T2* $n = 245$	Subjects with tau $n = 144$	Subjects with T2* and tau $n = 129$	p
Demographic characteristics					
Age, y, mean (SD)	78.0 (7.2)	77.7 (7.2)	78.2 (6.9)	78.0 (7.0)	0.918[a]
Sex, f/m, n	132/140	120/125	73/71	66/63	0.950[b]
CN/MCI, n	107/165	92/153	61/83	53/76	0.798[b]
APOE ε4, n (%)	91 (33.5%)	86 (35.1%)	47 (32.6%)	44 (34.1%)	0.963[b]
IFSH score, median (IQR)					
Right sulcus	1 (0–2)	1 (0–2)	1 (0–2)	1 (0–2)	0.497[c]
Central sulcus	1 (0–1)	1 (0–1)	1 (0–2)	1 (0–2)	0.340[c]
Left sulcus	1 (0–2)	1 (0–2)	1 (0–2)	1 (0–2)	0.542[c]
Total IFSH score	3 (0–6)	3 (0–6)	4 (1–6)	4 (1–6)	0.364[c]
SVD biomarkers					
PWMH Fazekas score, median (IQR)	1 (1–2)	1 (1–2)	1 (1–2)	1 (1–2)	0.981[c]
DWMH Fazekas score, median (IQR)	1 (1–2)	1 (1–2)	1 (1–2)	1 (1–1)	0.689[c]
PVS score BG, median (IQR)	3 (2–3)	3 (2–3)	3 (2–3)	3 (2–3)	0.975[c]
PVS score CSO, median (IQR)	3 (2–3)	3 (2–3)	3 (2–3)	3 (2–3)	0.993[c]
Microbleed, median (IQR)	/	0 (0–0)	/	0 (0–0)	0.450[d]
Lacune, median (IQR)	0(0–0)	0 (0–0)	0 (0–0)	0 (0–0)	0.713[c]
AD biomarkers					
Amyloid PET SUVR, mean (SD)	1.17 (0.24)	1.17 (0.24)	1.17 (0.24)	1.17 (0.24)	1.000[a]
Amyloid PET(+), n (%)	121 (44.5%)	110 (44.9%)	65 (45.1%)	58 (45.0%)	0.999[b]
tau PET SUVR, mean (SD)	/	/	1.30 (0.25)	1.31 (0.26)	0.752[a]
tau PET(+), n(%)	/	/	81 (56.3%)	74 (57.4%)	0.853[d]
BrainVol/TIV, mean (SD)	0.704 (0.002)	0.706 (0.002)	0.701 (0.003)	0.704 (0.003)	1.000[a]

[a]one-way ANOVA; [b]Chi-Squared Test; [c]Kruskal-Wallis test; [d]Mann-Whitney U test. *APOE*, apolipoprotein E; IFSH, inferior frontal sulcal hyperintensities; SVD, cerebral small vessel disease; IQR, interquartile range; PWMH, periventricular white matter hyperintensities; DWMH, deep white matter hyperintensities; PVS, perivascular spaces; BG, basal ganglia; CSO, centrum semiovale; AD, Alzheimer's disease; SUVR, Standardized Uptake Value Ratio.

Table 2
Associations between factors of interest and the IFSH score

	Model1 OR (95% CI)	Model2 OR (95% CI)	Model3 OR (95% CI)	Model4 OR (95% CI)
Age	1.00 (0.97 – 1.03)	1.01 (0.97 – 1.04)	1.01 (0.96 – 1.07)	0.94 (0.86 – 1.03)
Male Sex	1.19 (0.76 – 1.85)	1.20 (0.77 – 1.87)	0.84 (0.43 – 1.62)	0.55 (0.21 – 1.45)
APOE ε4	1.09 (0.69 – 1.75)	1.10 (0.69 – 1.77)	0.77 (0.37 – 1.59)	1.04 (0.37 – 2.87)
PWMH Fazekas score	1.22 (0.90 – 1.66)	1.24 (0.89 – 1.73)	1.49 (0.82 – 2.71)	1.61 (0.69 – 3.77)
DWMH Fazekas score	**1.75 (1.24 – 2.47)***	**1.79 (1.24 – 2.59)***	**2.16 (1.12 – 4.17)***	**3.02 (1.17 – 7.77)***
PVS score BG	1.25 (0.84 – 1.85)	1.25 (0.84 – 1.86)	0.96 (0.50 – 1.83)	0.40 (0.15 – 1.10)
PVS score CSO	1.09 (0.85 – 1.39)	1.08 (0.84 – 1.40)	1.23 (0.83 – 1.81)	**1.97 (1.09 – 3.57)***
Microbleed	1.14 (0.85 – 1.53)	1.16 (0.86 – 1.56)	0.87 (0.61 – 1.25)	0.76 (0.41 – 1.39)
Lacune	0.89 (0.62 – 1.29)	0.89 (0.61 – 1.30)	0.77 (0.37 – 1.60)	0.33 (0.11 – 1.04)
Amyloid PET SUVR	1.11 (0.44 – 2.85)	1.10 (0.42 – 2.84)	0.58 (0.13 – 2.47)	0.39 (0.05 – 2.92)
tau PET SUVR	1.00 (0.29 – 3.41)	0.97 (0.28 – 3.33)	/	1.38 (0.14 –13.69)
BrainVol/TIV[#]	**0.87 (0.81 – 0.92)***	**0.83 (0.77 – 0.90)***	**1.12 (1.00 – 1.25)***	1.06 (0.88 – 1.26)

*$p < 0.05$. Model1: univariate regression model. Model2: multivariable regression model, adjusted for age, and sex. Model3: multivariable regression model, the category of the IFSH score was set as the dependent variable, and age, sex, *APOE* ε4 genotype, SVD markers, Amyloid PET SUVR, BrainVol-to-TIV and scanners were set as independent variables. Model4: multivariable regression model, the category of the IFSH score was set as the dependent variable, age, sex, *APOE* ε4 genotype, SVD markers, BrainVol-to-TIV, AD biomarkers (including Amyloid PET SUVR and tau PET SUVR) and scanners were set as independent variables. Sample size: Models 1 & 2 were analyzed in the whole sample ($n = 272$) except for microbleed ($n = 245$), tau PET SUVR ($n = 144$); Model 3, $n = 245$; Model 4, $n = 129$. [#]the odd ratio represents changes induced by 1% of brain parenchymal fraction changes.

score and AD pathology markers. We noticed that the prevalence of IFSH was distinct in images produced by MR scanners from different manufacturers. However, the association between the DWMH and IFSH scores still existed after controlling for the MR manufacturers.

WMH is a common imaging abnormality during brain aging [20]. Although it is commonly considered

related to hypoxia and demyelination, evidence from recent studies suggests that glymphatic dysfunction may play a significant role [20, 21]. Various risk factors, such as hypertension, diabetes, and insomnia, can cause impaired glymphatic dysfunction during aging [22], leading to the stagnation of interstitial fluid and the occurrence of WMH. Indeed, many previous *in vivo* imaging studies suggest that WMH is associated with drastically increased water content [23]. Therefore, glymphatic dysfunction is a possible underlying mechanism supporting the association between WMH and IFSH. Notably, the IFSH score was associated with the DWMH but not the PWMH score. These findings may reflect that DWMH is more related to decreased peri-arterial fluid transport, the downstream of CSF flow in the subarachnoid space (including the inferior frontal sulcus). Our previous study found that DWMH lesions spatially connected to CSO-PVS, which are peri-arterial [24], and the volumes of DWMH and CSO-PVS were correlated [25]. The PWMH, on the other hand, maybe more related to hypoxia, venous disruption, and discontinuity of the ependyma lining [26, 27].

Although we hypothesized that the IFSH score might be related to AD biomarkers, no significant associations were found. One possible reason is the small sample number of subjects with tau PET data, which limited the detection of weak associations. While previous studies suggest that AD pathologies can cause vessel stiffness and neuroinflammation, which could decrease glymphatic function [28, 29], it is still unclear how strong these associations are. A lack of late-stage patients in the ADNI3 database is also a possible reason. Pathological damage may still be mild in the early disease stages. Due to the complexity of both AD and glymphatic function, this issue still needs further investigation.

We observed an association between the IFSH and CSO-PVS scores in model 4, but not in other statistical analyses. It seems that this association was not stable. Similarly, in Zhang's study, the associations were only significant in the whole sample but did not exist consistently among the three sub-cohorts. Specifically, the relationship between the PVS and IFSH scores was only seen in the MSS-3 group. Although the IFSH and dPVS are both imaging signs related to glymphatic clearance, they are in different sub-procedures. Furthermore, due to the complex associations between anatomical changes and fluid flow within tubular structures, a higher dPVS score does not necessarily reflect worse glymphatic clearance.

In univariate analysis, we found that subjects with lower brain parenchymal fractions had higher IFSH scores. Brain atrophy occurs during aging and various neurological disorders. It reflects a loss of neurons and fiber tracts in the whole brain, which is crucial for maintaining brain functions [30–32]. The death of neurons and glial cells may create abundant cell fragments and large molecules which need to be cleared out of the brain. During this process, some waste may deposit in the inferior frontal sulci. Nonetheless, the association diminished in multivariate models. In model 3, the confidential interval almost included 1, and the association was not significant in model 4. This is possibly due to the control of different scanner manufacturers.

This study is subject to several limitations. Firstly, there are no T2 images in the ADNI3 database, so we used T1 images to evaluate dPVS. While evaluation based on T2 images is more sensitive, T1 images have also been widely used for dPVS evaluation and the results showed robust associations with clinical variables [17]. Secondly, the sample size of patients with tau-PET data was relatively small. Thirdly, this is a cross-sectional study, so a causal relationship between IFSH and other variables could not be determined. Finally, as IFSH is a newly proposed imaging sign, the influence of imaging artifacts cannot be ruled out. Despite a distinct prevalence of IFSH in images from different manufacturers, the association between IFSH and DWMH still existed after controlling the manufacturer. It is true pathophysiological meanings still need to be validated in future pathology studies and clinical investigations in cohorts with different neurological diseases.

ACKNOWLEDGMENTS

Data collection and sharing for this project was funded by the Alzheimer's Disease Neuroimaging Initiative (ADNI) (National Institutes of Health Grant U01 AG024904) and DOD ADNI (Department of Defense award number W81XWH-12-2-0012). ADNI is funded by the National Institute on Aging, the National Institute of Biomedical Imaging and Bioengineering, and through generous contributions from the following: AbbVie, Alzheimer's Association; Alzheimer's Drug Discovery Foundation; Araclon Biotech; BioClinica, Inc.; Biogen; Bristol-Myers Squibb Company; CereSpir, Inc.; Cogstate; Eisai Inc.; Elan Pharmaceuticals, Inc.; Eli Lilly and Company; EuroImmun; F. Hoffmann-La Roche Ltd

and its affiliated company Genentech, Inc.; Fujirebio; GE Healthcare; IXICO Ltd.; Janssen Alzheimer Immunotherapy Research & Development, LLC.; Johnson & Johnson Pharmaceutical Research & Development LLC.; Lumosity; Lundbeck; Merck & Co., Inc.; Meso Scale Diagnostics, LLC.; NeuroRx Research; Neurotrack Technologies; Novartis Pharmaceuticals Corporation; Pfizer Inc.; Piramal Imaging; Servier; Takeda Pharmaceutical Company; and Transition Therapeutics. The Canadian Institutes of Health Research is providing funds to support ADNI clinical sites in Canada. Private sector contributions are facilitated by the Foundation for the National Institutes of Health (http://www.fnih.org). The grantee organization is the Northern California Institute for Research and Education, and the study is coordinated by the Alzheimer's Therapeutic Research Institute at the University of Southern California. ADNI data are disseminated by the Laboratory for Neuro Imaging at the University of Southern California.

FUNDING

This study was funded by the Natural Science Foundation of Zhejiang Province (Grant No. LSZ19H180001 PH and LQ20H180015 RZ), the National Natural Science Foundation of China (Grant Nos. 82101987 RZ), the China Postdoctoral Science Foundation (Grant No. 2019M662083 RZ) and the Zhejiang province Postdoctoral Science Foundation.

CONFLICT OF INTEREST

The authors have no conflict of interest to report.

DATA AVAILABILITY

The data used in this study were from the Alzheimer's disease Neuroimaging Initiative (ADNI) database: http://adni.loni.usc.edu/.

SUPPLEMENTARY MATERIAL

The supplementary material is available in the electronic version of this article: https://dx.doi.org/10.3233/JAD-220843.

REFERENCES

[1] Lee H, Kim E, Lee KM, Kim JH, Bae YJ, Choi BS, Jung C (2015) Clinical implications of sulcal enhancement on postcontrast fluid attenuated inversion recovery images in patients with acute stroke symptoms. *Korean J Radiol* **16**, 906-913.

[2] Oshida S, Akamatsu Y, Matsumoto Y, Ishigame S, Ogasawara Y, Aso K, Kashimura H (2019) A case of chronic subdural hematoma demonstrating the epileptic focus at the area with sulcal hyperintensity on fluid-attenuated inversion recovery image. *Radiol Case Rep* **14**, 1109-1112.

[3] Melhem ER, Jara H, Eustace S (1997) Fluid-attenuated inversion recovery MR imaging: Identification of protein concentration thresholds for CSF hyperintensity. *AJR Am J Roentgenol* **169**, 859-862.

[4] Benveniste H, Liu X, Koundal S, Sanggaard S, Lee H, Wardlaw J (2019) The glymphatic system and waste clearance with brain aging: A review. *Gerontology* **65**, 106-119.

[5] Zhang JF, Lim HF, Chappell FM, Clancy U, Wiseman S, Valdés-Hernández MC, Garcia DJ, Bastin ME, Doubal FN, Hewins W, Cox SR, Maniega SM, Thrippleton M, Stringer M, Jardine C, McIntyre D, Barclay G, Hamilton I, Kesseler L, Murphy M, Perri CD, Wu YC, Wardlaw JM (2021) Relationship between inferior frontal sulcal hyperintensities on brain MRI, ageing and cerebral small vessel disease. *Neurobiol Aging* **106**, 130-138.

[6] Wardlaw JM, Benveniste H, Nedergaard M, Zlokovic BV, Mestre H, Lee H, Doubal FN, Brown R, Ramirez J, MacIntosh BJ, Tannenbaum A, Ballerini L, Rungta RL, Boido D, Sweeney M, Montagne A, Charpak S, Joutel A, Smith KJ, Black SE (2020) Perivascular spaces in the brain: Anatomy, physiology and pathology. *Nat Rev Neurol* **16**, 137-153.

[7] Weller RO, Djuanda E, Yow HY, Carare RO (2009) Lymphatic drainage of the brain and the pathophysiology of neurological disease. *Acta Neuropathol* **117**, 1-14.

[8] Albayram MS, Smith G, Tufan F, Tuna IS, Bostancıklıoğlu M, Zile M, Albayram O (2022) Non-invasive MR imaging of human brain lymphatic networks with connections to cervical lymph nodes. *Nat Commun* **13**, 203.

[9] Li Y, Rusinek H, Butler T, Glodzik L, Pirraglia E, Babich J, Mozley PD, Nehmeh S, Pahlajani S, Wang X, Tanzi EB, Zhou L, Strauss S, Carare RO, Theise N, Okamura N, de Leon MJ (2022) Decreased CSF clearance and increased brain amyloid in Alzheimer's disease. *Fluids Barriers CNS* **19**, 21.

[10] Braak H, Braak E (1991) Neuropathological stageing of Alzheimer-related changes. *Acta Neuropathol* **82**, 239-259.

[11] Iqbal K, Alonso Adel C, Chen S, Chohan MO, El-Akkad E, Gong CX, Khatoon S, Li B, Liu F, Rahman A, Tanimukai H, Grundke-Iqbal I (2005) Tau pathology in Alzheimer disease and other tauopathies. *Biochim Biophys Acta* **1739**, 198-210.

[12] Kim HW, Hong J, Jeon JC (2020) Cerebral small vessel disease and Alzheimer's disease: A review. *Front Neurol* **11**, 927.

[13] Hansson O (2021) Biomarkers for neurodegenerative diseases. *Nat Med* **27**, 954-963.

[14] Bubu OM, Brannick M, Mortimer J, Umasabor-Bubu O, Sebastião YV, Wen Y, Schwartz S, Borenstein AR, Wu Y, Morgan D, Anderson WM (2017) Sleep, cognitive impairment, and Alzheimer's disease: A systematic review and meta-analysis. *Sleep* **40**, doi: 10.1093/sleep/zsw032

[15] Villemagne VL, Rowe CC (2013) Long night's journey into the day: Amyloid-β imaging in Alzheimer's disease. *J Alzheimers Dis* **33**(Suppl 1), S349-359.

[16] Wardlaw JM, Benveniste H, Williams A (2022) Cerebral vascular dysfunctions detected in human small vessel disease and implications for preclinical studies. *Annu Rev Physiol* **84**, 409-434.

[17] Zhu YC, Dufouil C, Mazoyer B, Soumaré A, Ricolfi F, Tzourio C, Chabriat H (2011) Frequency and location of dilated Virchow-Robin spaces in elderly people: A population-based 3D MR imaging study. *AJNR Am J Neuroradiol* **32**, 709-713.

[18] Fazekas F, Chawluk JB, Alavi A, Hurtig HI, Zimmerman RA (1987) MR signal abnormalities at 1.5 T in Alzheimer's dementia and normal aging. *AJR Am J Roentgenol* **149**, 351-356.

[19] Lim HF, Zhang J-F, Wardlaw J (2021) User guide for Inferior Frontal Sulcal Hyperintensity (IFSH) Scale and related template.

[20] Ding T, Cohen AD, O'Connor EE, Karim HT, Crainiceanu A, Muschelli J, Lopez O, Klunk WE, Aizenstein HJ, Krafty R, Crainiceanu CM, Tudorascu DL (2020) An improved algorithm of white matter hyperintensity detection in elderly adults. *Neuroimage Clin* **25**, 102151.

[21] Sabayan B, Westendorp RGJ (2021) Neurovascular-glymphatic dysfunction and white matter lesions. *Geroscience* **43**, 1635-1642.

[22] Nedergaard M, Goldman SA (2020) Glymphatic failure as a final common pathway to dementia. *Science* **370**, 50-56.

[23] Merino JG (2019) White matter hyperintensities on magnetic resonance imaging: What is a clinician to do? *Mayo Clin Proc* **94**, 380-382.

[24] Bouvy WH, Biessels GJ, Kuijf HJ, Kappelle LJ, Luijten PR, Zwanenburg JJ (2014) Visualization of perivascular spaces and perforating arteries with 7 T magnetic resonance imaging. *Invest Radiol* **49**, 307-313.

[25] Huang P, Zhang R, Jiaerken Y, Wang S, Yu W, Hong H, Lian C, Li K, Zeng Q, Luo X (2021) Deep white matter hyperintensity is associated with the dilation of perivascular space. *J Cereb Blood Flow Metab* **41**, 2370-2380.

[26] Zhang R, Huang P, Jiaerken Y, Wang S, Hong H, Luo X, Xu X, Yu X, Li K, Zeng Q (2021) Venous disruption affects white matter integrity through increased interstitial fluid in cerebral small vessel disease. *J Cereb Blood Flow Metab* **41**, 157-165.

[27] Fazekas F, Kleinert R, Offenbacher H, Schmidt R, Kleinert G, Payer F, Radner H, Lechner H (1993) Pathologic correlates of incidental MRI white matter signal hyperintensities. *Neurology* **43**, 1683-1683.

[28] Mestre H, Tithof J, Du T, Song W, Peng W, Sweeney AM, Olveda G, Thomas JH, Nedergaard M, Kelley DH (2018) Flow of cerebrospinal fluid is driven by arterial pulsations and is reduced in hypertension. *Nat Commun* **9**, 4878.

[29] Zeng Q, Li K, Luo X, Wang S, Xu X, Jiaerken Y, Liu X, Hong L, Hong H, Li Z, Fu Y, Zhang T, Chen Y, Liu Z, Huang P, Zhang M (2022) The association of enlarged perivascular space with microglia-related inflammation and Alzheimer's pathology in cognitively normal elderly. *Neurobiol Dis* **170**, 105755.

[30] Vibha D, Tiemeier H, Mirza SS, Adams HHH, Niessen WJ, Hofman A, Prasad K, van der Lugt A, Vernooij MW, Ikram MA (2018) Brain volumes and longitudinal cognitive change: A population-based study. *Alzheimer Dis Assoc Disord* **32**, 43-49.

[31] Fjell AM, Walhovd KB (2010) Structural brain changes in aging: Courses, causes and cognitive consequences. *Rev Neurosci* **21**, 187-221.

[32] Schirmer MD, Donahue KL, Nardin MJ, Dalca AV, Giese AK, Etherton MR, Mocking SJT, McIntosh EC, Cole JW, Holmegaard L, Jood K, Jimenez-Conde J, Kittner SJ, Lemmens R, Meschia JF, Rosand J, Roquer J, Rundek T, Sacco RL, Schmidt R, Sharma P, Slowik A, Stanne TM, Vagal A, Wasselius J, Woo D, Bevan S, Heitsch L, Phuah CL, Strbian D, Tatlisumak T, Levi CR, Attia J, McArdle PF, Worrall BB, Wu O, Jern C, Lindgren A, Maguire J, Thijs V, Rost NS (2020) Brain volume: An important determinant of functional outcome after acute ischemic stroke. *Mayo Clin Proc* **95**, 955-965.